Introduction to Permanent Magnet Motor Control

Abstract

This document introduces 3-phase permanent magnet motors, briefly explaining the construction and differences between brushless DC and permanent magnet synchronous machines. The ubiquitous three-phase, two-level voltage source inverter is introduced along with its switch state map. A look inside a Qorvo motor control & driver reveals all the function blocks needed for any type of motor or inverter control. The concepts of trapezoidal commutation with and without rotor position sensing is followed by a high-level explanation of field-oriented control. Understanding the tradeoffs of each control method helps to optimize motorized applications.

1. Introduction

The popularity of permanent magnet (PM) motors is easy to understand. Synchronous operation with its precise speed and position capability, seamless transition between motoring a regenerative braking, and high efficiency make these motors an obvious choice for applications ranging from fractional kilowatts to hundreds of kilowatts. Not so easy to understand are the intricate control system details of a brushless DC (BLDC) or permanent magnet synchronous machine (PMSM), also called permanent magnet synchronous motor although it also functions as a generator. This application note provides a functional overview of these two motor types and their common control methods. Salient-pole (stepper) motors are excluded. The intent is to provide enough information to make informed decisions about which motor type and control approach is optimum for various applications.

2. PM Motor Drive System

When using an integrated motor controller & driver (MCD), a PM drive system reduces to four building blocks: First, a variety of power source options, second, the MCD with integrated microcontroller (MCU), third, a 3-phase inverter, and fourth, the PM motor.

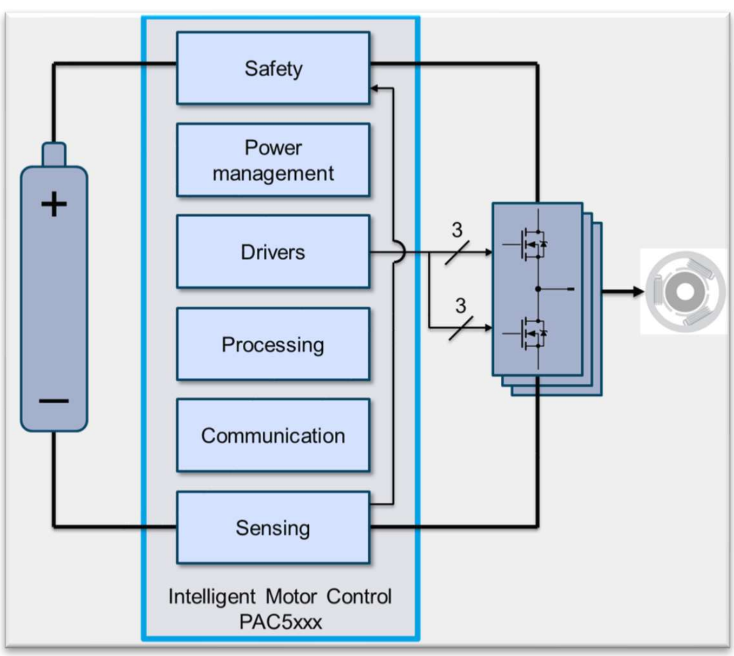

Fig. 2-1. Four building blocks of a PM motor drive system

The power source can be a battery pack or an AC-to-DC power supply. The power source in Fig. 2-1 is a battery pack. A highly integrated MCD such as Qorvo PAC55xxx series or ACT72350 with separate MCU greatly simplifies the motor drive system design and saves considerable cost and circuit board area by integrating multiple functions into a single integrated circuit, as indicated in Fig. 2-1. The inverter is almost always three half-bridges. This type of inverter is called 2-level voltage source, or 2L-VSI for short. Each half-bridge has two series-connected switch positions, with the center point of each half-bridge connected to a motor terminal. Each switch position is usually a power MOSFET, or multiple parallel power MOSFETs. Finally, there is the PM motor. Each system building block is described in more detail.

2.1. Power Source

2.1.1. Battery Pack

A modern battery pack is usually lithium-based. The focus here is on applications with anywhere from 3 to 20 series cells, or a nominal battery pack voltage from 9 to 80 V. More information about battery packs, battery-powered applications, and battery management systems is found in [1] and [2].

2.1.2. AC-DC Converter

Regenerative braking converts mechanical power to electrical power flowing back into the AC supply source. This requires bidirectional power capability in the AC-DC converter. To accomplish this, the AC-DC converter must contain at least two half-bridges in its rectifier stage and its DC-DC converter stage. Topologies with diode bridges will not work, such as a single-phase diode bridge followed by a power factor correction (PFC) boost converter, a 3-phase diode bridge, or a 3-phase Vienna rectifier. Single-phase AC-DC topologies that have bidirectional capability are commonly called bridgeless, meaning *diode* bridgeless. A common example is a totem-pole PFC (TPPFC). 3-phase examples include 2L-VSI, or T-type neutral point clamped (TNPC) inverter, each operated with -1 power factor (rectifier mode). Bidirectional DC-DC converters include CLLC, dual active bridge (DAB), and full-bridge, for example.

2.2. Integrated Motor Controller & Driver

Qorvo Power Application Controller® (PAC) PAC55xxx series are highly integrated and optimized for motion control. These include a 150 MHz Arm® Cortex®-M4F 32-bit microcontroller core with floating point unit (FPU), hardware multiply/divide, 128 KB of FLASH, and 32 KB of SRAM. The Configurable Analog Front End (CAFE) shown in Fig. 2-2 contains precision differential and single-ended programmable-gain amplifiers for current and other sensing, and multiple function-specific protection comparators with dedicated digital-to-analog converters (DAC). The extremely fast analog-to-digital converter (ADC), and hardware multiply & divide in each PAC55xx MCD minimize delay-induced errors in control calculations. If rotor position sensing is needed, such as in high-precision positioning, the QEP module decodes rotor quadrature encoder signals. The pulse width modulation (PWM) generator is the PWM & deadtime block. It includes safety logic from overcurrent comparators and other sources. The integrated power manager powers the high-side and low-side gate drivers and all internal circuitry.

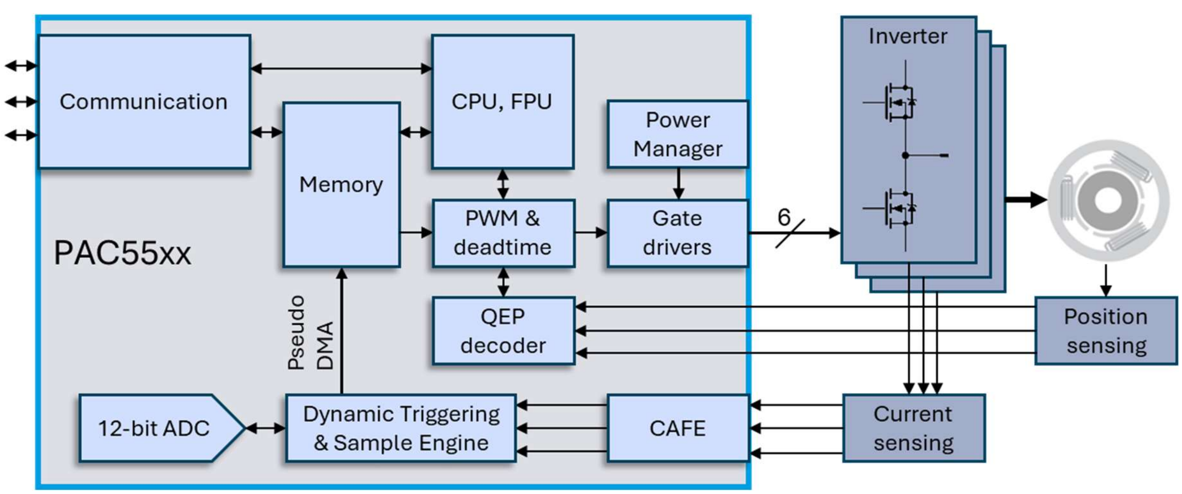

Fig. 2-2 PAC55xxx MCD in a motor drive system

2.3. Inverter

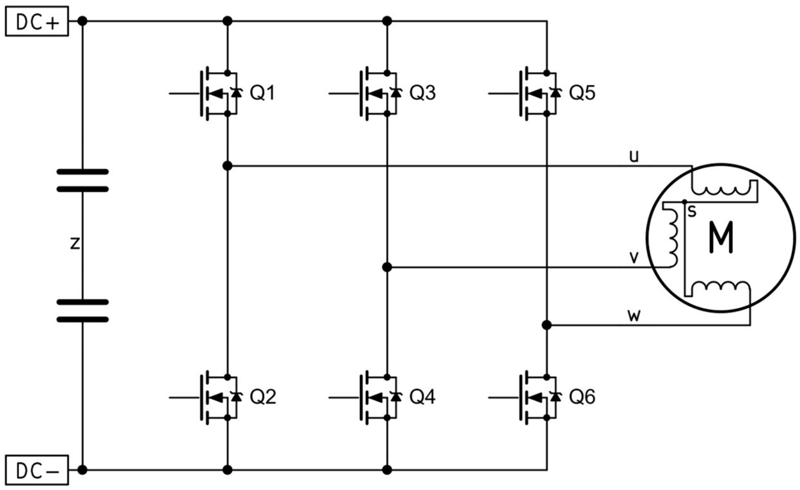

Fig. 2-3. 2L-VSI inverter and permanent magnet motor

Fig. 2-3 shows a 2L-VSI connected to a synchronous permanent magnet motor, which could be either BLDC or PMSM. Some definitions are required before discussing control details. The inverter power source is the DC link, labelled DC+ and DC- in Fig. 2-3. The notation for the total DC link voltage from DC- to DC+ is V_{bus}. The DC link is “voltage stiff”, supported by a capacitor bank that supplies or absorbs high frequency ripple currents that are a normal aspect of inverter operation. The capacitor bank in Fig. 2-3 is drawn split with center point labeled ‘z’, however the capacitor bank of a 2-level inverter need not be split, and the DC link voltage for a PM motor drive is generally not so high to require series-connecting capacitors. Therefore, point z is usually virtual but is included as a voltage reference point for control voltages. Positive phase current flows into the corresponding motor terminal. The node labelled ‘s’ in the PM motor is the star-connected midpoint of the three stator windings.

Safe operation of a 2L-VSI is governed by two simple rules:

1. The switches in each half-bridge must never conduct simultaneously.
2. Each switch must allow reverse current to flow regardless of whether the switch is on or off.

The first rule prevents shorting the DC link, which would cause catastrophic failure due to rapid overheating of the half-bridge switches. The second rule allows continuous current flow through the inductive load (motor windings) regardless of inverter switching. When one switch in a half-bridge switches off, there is a short deadtime when both half-bridge switches are off. Current can “freewheel” (flow in the reverse direction) through the other switch that subsequently switches on after the deadtime. Interlock and deadtime generation are configurable and automatically implemented in Qorvo MCDs.

The body diode of a MOSFET fulfills the second rule without requiring an additional diode. The high performance of silicon and silicon-carbide power MOSFETs make them attractive for inverters.

2.4. Permanent Magnet Motors

Fig. 2-4(a) shows a partially disassembled PMSM, and (b) shows a BLDC external rotor with magnets. The construction of PMSM and BLDC motors is similar, but there are some key differences that affect their control strategy.

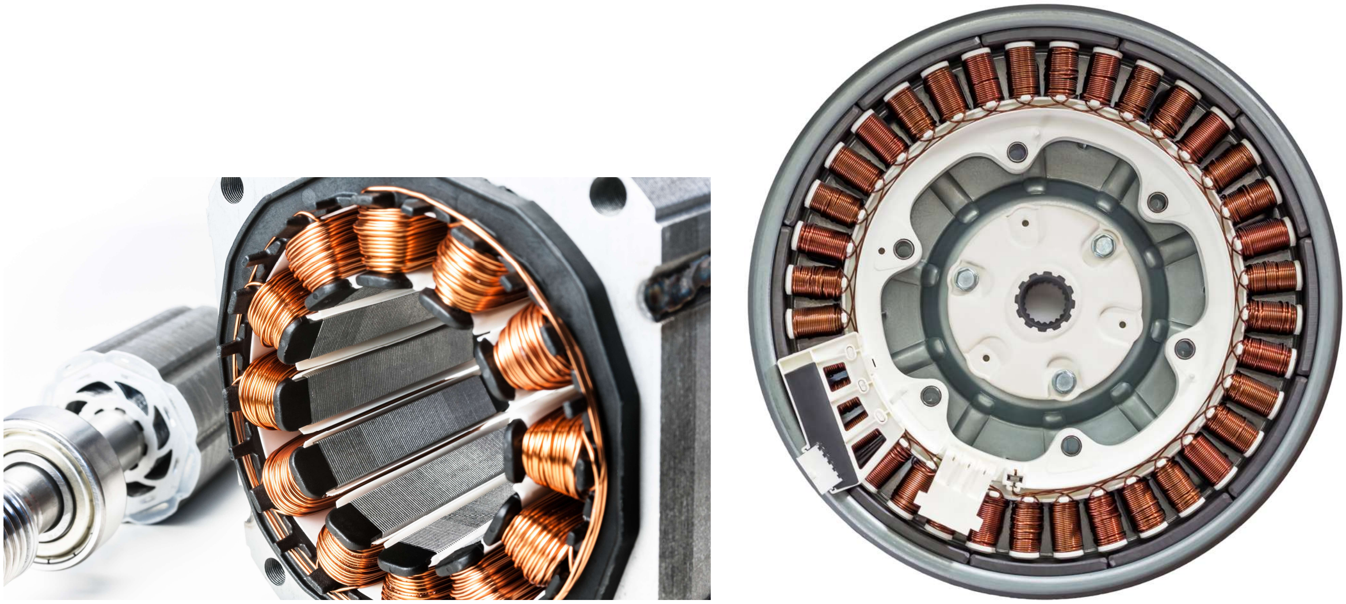

(a) (b)

Fig. 2-4. (a) Disassembled PMSM, and (b) BLDC with external rotor

For both PMSM and BLDC, there are three stator windings, thus they are 3-phase machines. These windings connect inside the motor, and the other end of each winding is brought out to terminals that connect to the inverter. The center connection point inside is labelled 's' in Fig. 2-3 and is generally inaccessible. The windings are distributed across multiple "poles", as shown in Fig. 2-4. Windings sometime share a pole. BLDC windings are concentrated, whereas PMSM windings are more distributed by varying the number of turns each winding has on shared poles. Furthermore, the shape of the magnets is often different, with PMSM magnets having rounded edges, whereas BLDC magnets have rectangular cross section.

As the rotor spins, the magnets moving past the poles creates a changing magnetic field in the windings. According to the Faraday-Lenz law, this creates an electromotive force (EMF), or back-EMF (BEMF) that tends to oppose the change in a magnetic field. If you measure the voltage across two motor terminals and spin the rotor, the resulting waveform for a BLDC motor is roughly trapezoidal, and for a PMSM it is roughly sinusoidal. The goal of each motor design is to match the BEMF waveform with the control strategy, known as commutation method, one being trapezoidal for BLDC, and the other sinusoidal for PMSM.

The relationship between BEMF and rotor speed is $E_b = \omega \cdot K_e$, where E_b is BEMF, ω is the rotor angular velocity, and K_e is a constant that depends on the motor design and is commonly in Volts per RPM. In motor mode where electrical energy converts to torque, BEMF limits motor current, among other things. In generator mode, it is BEMF that forces current into the power source as torque converts to electrical energy. This relationship explains why motor current during startup is much higher than at operating speed. A second (simplified) relationship is between current and torque: $T = K_t \cdot I_q$, where K_t is a motor constant, and I_q is torque-generating motor current.

3. Trapezoidal Control of a BLDC Motor

Trapezoidal commutation is simple but also quite different from other 3-phase control methods because only two of the three stator windings are energized at any given time. Furthermore, it is driven with DC rather than AC currents.

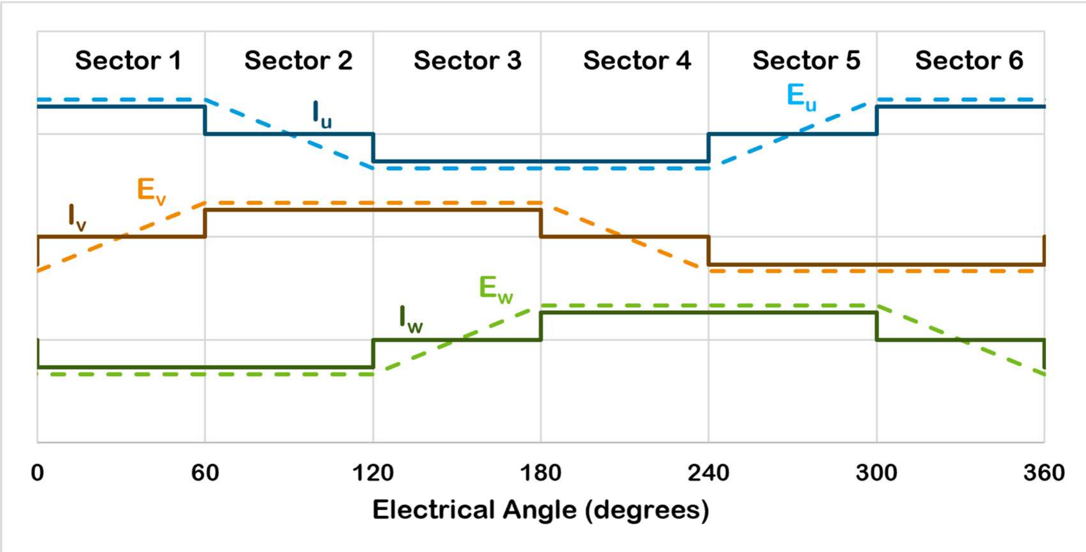

Fig. 3-1. BLDC idealized BEMF and current waveforms versus electrical angle

Fig. 3-1 shows idealized phase BEMF and current waveforms for each winding of a running BLDC motor, and it is clear why trapezoidal commutation is also called six-step or block commutation. In this approach, the electrical cycle is divided into six discrete 60-degree sectors, with each phase being either energized or left floating in a specific sequence. This creates three possible current paths through the motor windings, with the active current path changing every 60 electrical degrees based on rotor position. The resulting voltage waveforms approximate trapezoidal shapes, giving this method its name. Measuring the time required to traverse a sector enables calculation of rotational speed. Here we note that rotor angle equals electrical angle divided by the number of rotor pole pairs. Motor control uses electrical angle, which is derived from rotor position measurement or by sensorless estimation techniques.

BLDC rotor position is usually sensed with three embedded Hall-effect sensors positioned 120 degrees apart. The output of each Hall-effect sensor is a binary signal. The controller uses a lookup table to map the sensor states to the corresponding commutation sector, ensuring that the stator magnetic fluxes align with the rotor for maximum torque per stator current. This approach is straightforward to implement and provides reliable operation, even during startup and low speed operation. The inclusion of physical sensors adds a little cost, some wiring, and connectors.

Sensorless control relies on detecting the zero-crossings of the BEMF generated in the unenergized phase. The controller monitors the motor voltages (usually from each terminal to system ground) and identifies the appropriate instant to advance the commutation sequence. This method reduces cost and increases reliability. However, sensorless commutation requires rotation to generate BEMF, making it difficult to start the motor under load.

The magnitude of the motor current in each 60-degree sector is regulated by PWM. The PWM duty cycle is not changing with an AC fundamental waveform but rather based on steady-state speed or torque control. This greatly simplifies BLDC control but note that neither the inverter nor the motor is fully utilized. Only two inverter legs are active at a time, never all three. With both phase leg switch positions off, the unenergized phase voltage floats based on BEMF.

Fig. 3-1 shows idealized waveforms. Real current waveforms have notches and rounded corners in the current. Also, BEMF is never purely trapezoidal; it has rounded corners and peaks, a mix between trapezoidal and sinusoidal shape. These artifacts create torque ripple, which is a disadvantage for precise speed or position control. For many applications however, some torque ripple is inconsequential.

Three PWM methods are described next, first bipolar, then unipolar with inverted control, and finally unipolar with two carriers.

3.1. PWM with Bipolar Switching

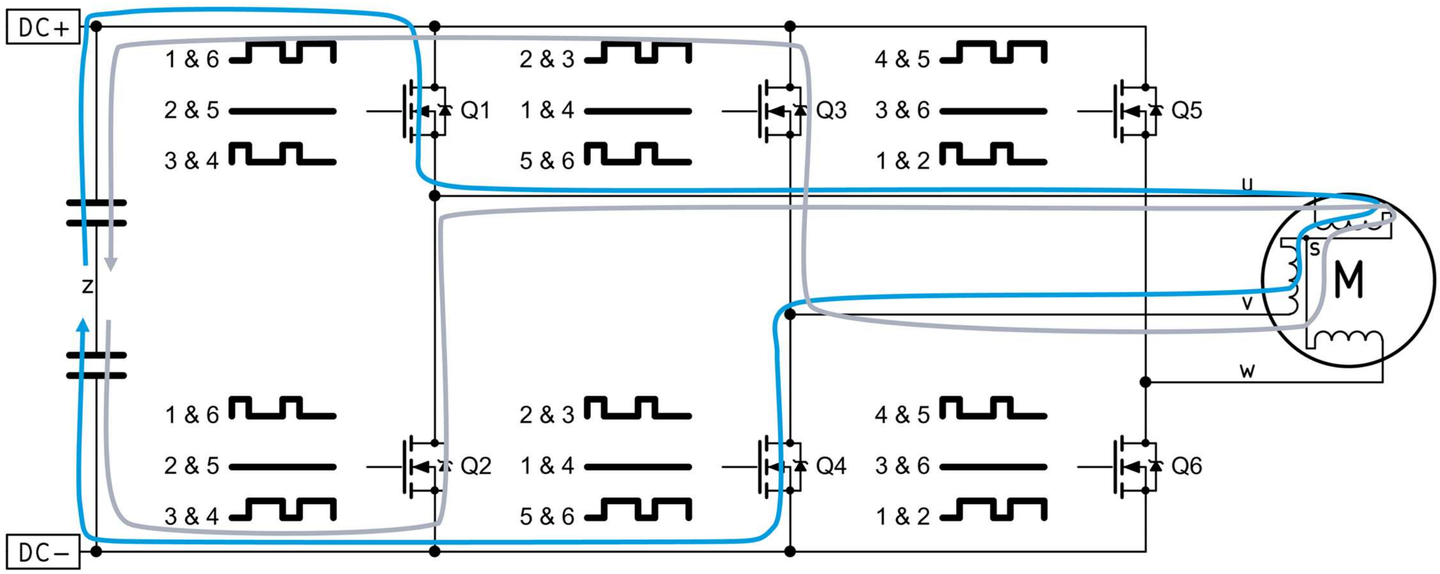

Fig. 3-2. 2L-VSI showing bipolar PWM gate control scheme by sector number and currents during one switching cycle in sector 6

With trapezoidal commutation, a BLDC motor is always driven by an H-bridge because at any given time, one leg of the inverter is idle; it has both switches off. Whether an inverter leg is included in the H-bridge or is idle depends on the sector. Fig. 3-2 shows phase *u* and *v* forming the H-bridge and phase *w* idle, corresponding to operation in sector 6. The MOSFETs in the H-bridge switch at much higher frequency than the winding currents can significantly respond. Switching frequency is in the range of thousands to tens of thousands of cycles per second.

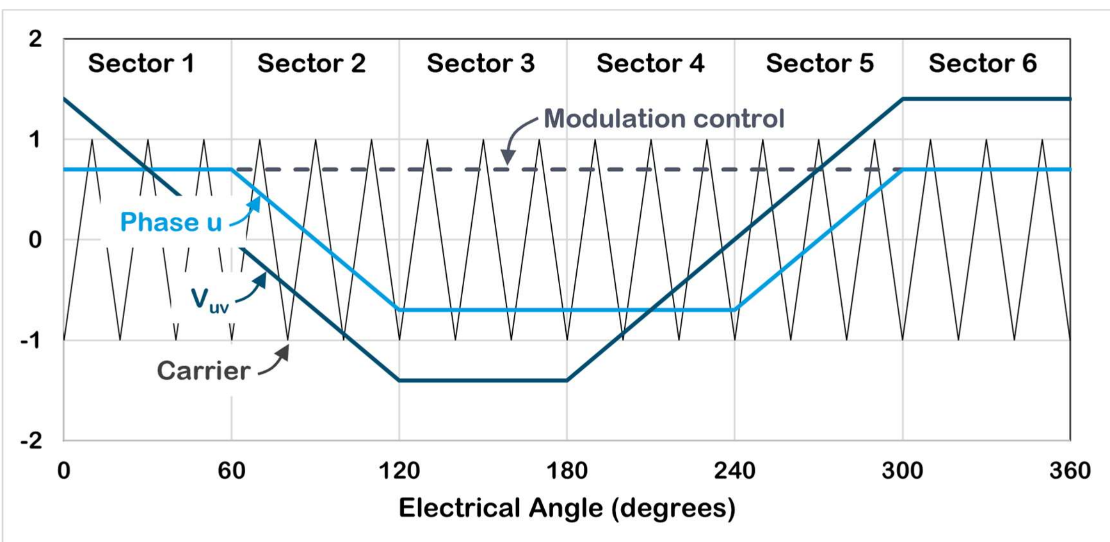

Fig. 3-3. Bipolar modulation control and carrier waveforms, scaled phase *u* BEMF and scaled *u* – *v* machine terminal voltage

Fig. 3-3 shows a modulation control signal (dashed line, also known as reference voltage) superimposed upon a triangular, switching-frequency carrier waveform, which is typical of PWM generation. (The carrier frequency in Fig. 3-3 is artificially low for clarity.) With bipolar PWM for BLDC, the normalized carrier waveform spans from -1 to +1, and the DC, normalized modulation control also spans from -1 to +1. (In the MCU, the triangle waveform is implemented with a PWM up-down counter.) Fig. 3-3 also shows the phase *u* voltage, again with respect to point *z* in Fig. 3-2, normalized to the same scale as the modulation control signal. The line-to-line (motor terminal-to-terminal) voltage between *u* and *v* terminals is also shown with the same scaling. Note the larger magnitude and 30-degree shift compared to the phase voltage.

Considering sector 6, when the modulation control signal is greater than the carrier waveform, then switch Q1 and Q4 in Fig. 3-2 are gated on while Q2 and Q3 are always gated the opposite. The DC link voltage applies across phase *u* and *v* stator windings in series, causing current to increase along the path indicated by the blue line in Fig. 3-2. The *w* motor terminal floats because Q5 and Q6 remain off, and the *w* terminal voltage with respect to virtual point ***z*** crosses zero amid sector 6. As the carrier waveform rises above the modulation control, then Q1 and Q4 switch off, and after a short deadtime Q2 and Q3 switch on. This applies a negative DC link voltage across motor terminals *u* and *v*, which consequently encounter a voltage swing of twice the DC link voltage. The motor terminals are driven to plus and minus the DC link voltage ($\pm V_{bus}$), which is why this is called bipolar switching. Winding inductances cause current to flow continuously, but the inverse DC link voltage reduces its magnitude. The motor current is therefore DC with triangular ripple at the switching frequency.

Here we introduce the concept of a switching function $\tau(t)$, which is a function of the pulse pattern to control the switches in the inverter. When $\tau(t) = 1$ a corresponding MOSFET is gated on, and the MOSFET is gated off when $\tau(t) = 0$. $\tau(t)$ includes a modulation function, which is simply the modulation factor *M* for DC control. With this inclusion, the bipolar PWM duty equation is $\tau = \frac{1}{2} \cdot (1 + M)$, where *M* is the ratio of the modulation control voltage to the peak of the triangle carrier waveform, as indicated in Fig. 3-3, which has *M* = 0.7. We note that if *M* = 0, the switches in sector 6 H-bridge of Fig. 3-2 are on half the time (50% duty, ignoring deadtime), and that the average phase voltage is zero. In other words, with the rotor at a standstill, 50% duty results in no net phase current and zero torque, and no power flow. With *M* < 0, phase current flows in the opposite direction and torque reverses.

3.2. PWM with Unipolar Switching, Two Control Signals

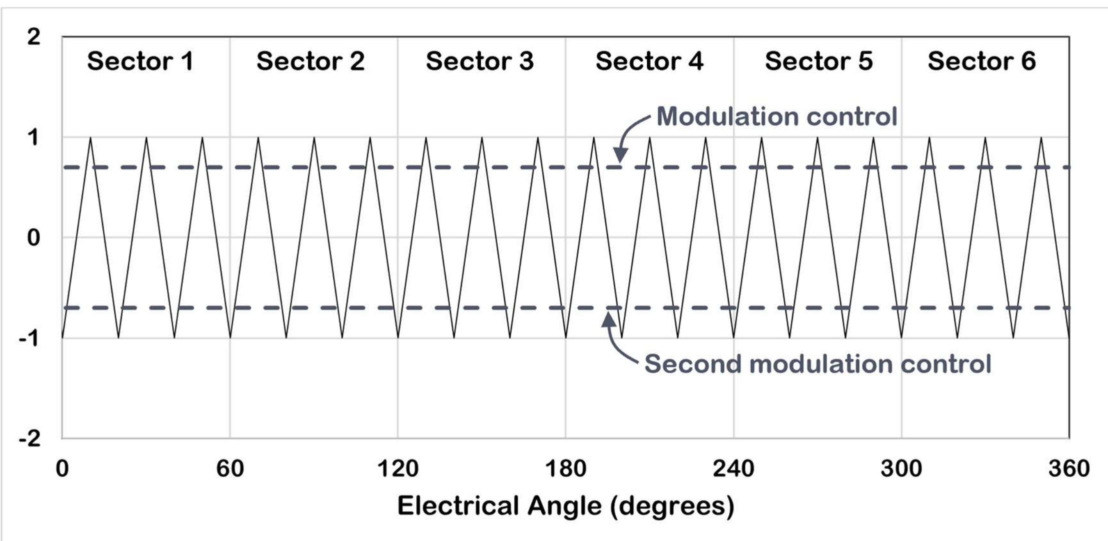

Fig. 3-4. Unipolar switching with two modulation controls and one carrier waveform

Now we imagine adding a second modulation control signal as in Fig. 3-4. This signal is simply a negative copy of the original modulation control signal. In sector 6, the original control signal controls Q1 as with bipolar switching, with Q2 always switched the opposite of Q1. Similarly, the negated control signal controls Q2 with Q3 switched the opposite. With this method, both Q1 and Q3, or Q2 and Q4 can be on simultaneously, resulting in zero volts across terminals *u* and *v* (ignoring the small voltage drop across conducting MOSFETs). This results in line-to-line voltage V_{uv} alternating between 0 and DC+, significantly reducing the ripple voltage compared to bipolar switching. The PWM duty equation is the same as for bipolar switching, and so is the power loss in the inverter. This modulation method doubles the switching frequency at the motor terminals. Pulse widths at the PM motor become very narrow as the PWM duty approaches 50%. This is inefficient for the PM motor, so minimum pulse width restrictions could be imposed. If the modulation controls cross zero, the phase current flows in the opposite direction and torque reverses.

3.3. PWM with Unipolar Switching, Two Carriers

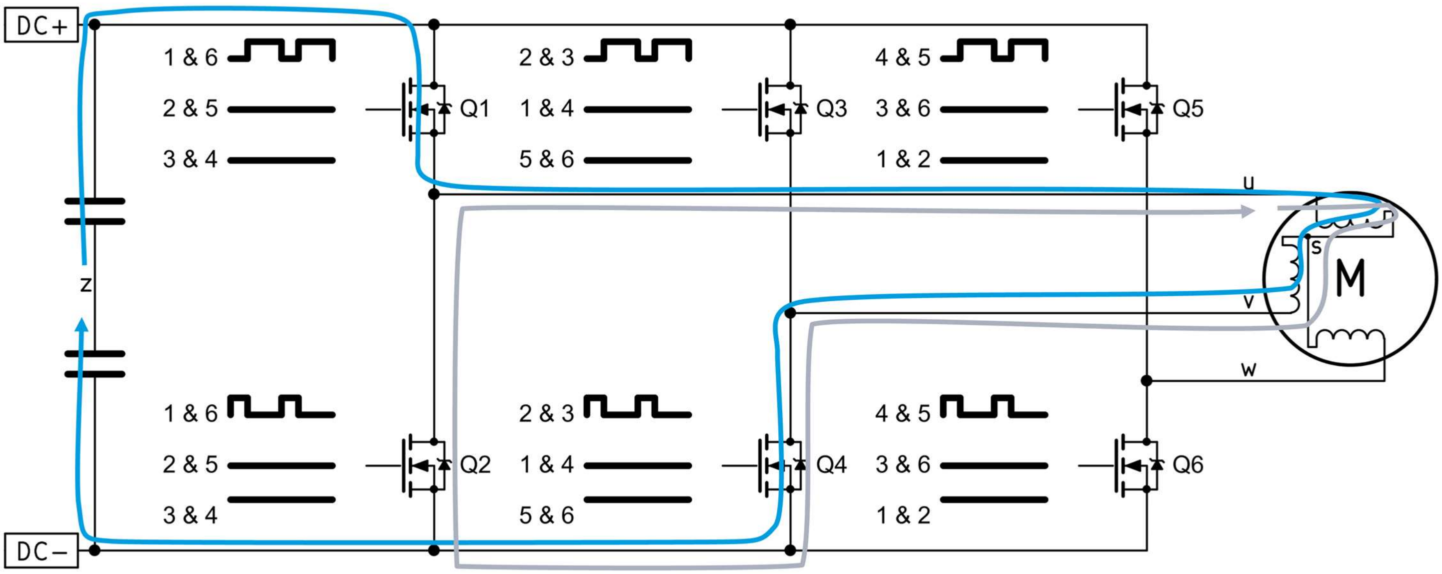

Fig. 3-5. 2L-VSI showing unipolar PWM gate control by sector number and currents during one switching cycle in sector 6

Finally, we have a single modulation control and two carriers as shown in Fig. 3-6. In sector 6, Q1 is on whenever the modulation control is greater than the top carrier, and Q2 switches opposite of Q1 as always. Similarly, Q4 is on whenever the modulation control is greater than the *bottom* carrier, with Q3 switching opposite of Q4. Fig. 3-5 shows one switching cycle in sector 6. As before, the DC link voltage applies across phase *u* and *v* stator windings in series, causing current to increase along the path indicated by the blue line in Fig. 3-5. The *w* motor terminal floats because Q5 and Q6 remain off, and the *w* terminal voltage with respect to virtual point *z* crosses zero amid sector 6. As the carrier waveform rises above the modulation control, then Q1 switches off, and after a short deadtime Q2 switches on. At this point, both Q2 and Q4 are on, shorting motor terminals *u* and *v*. The line-to-line voltage swings between 0 and DC+, with much lower ripple voltage than bipolar switching has. If the modulation control is negative, the phase current flows in the opposite direction and torque reverses.

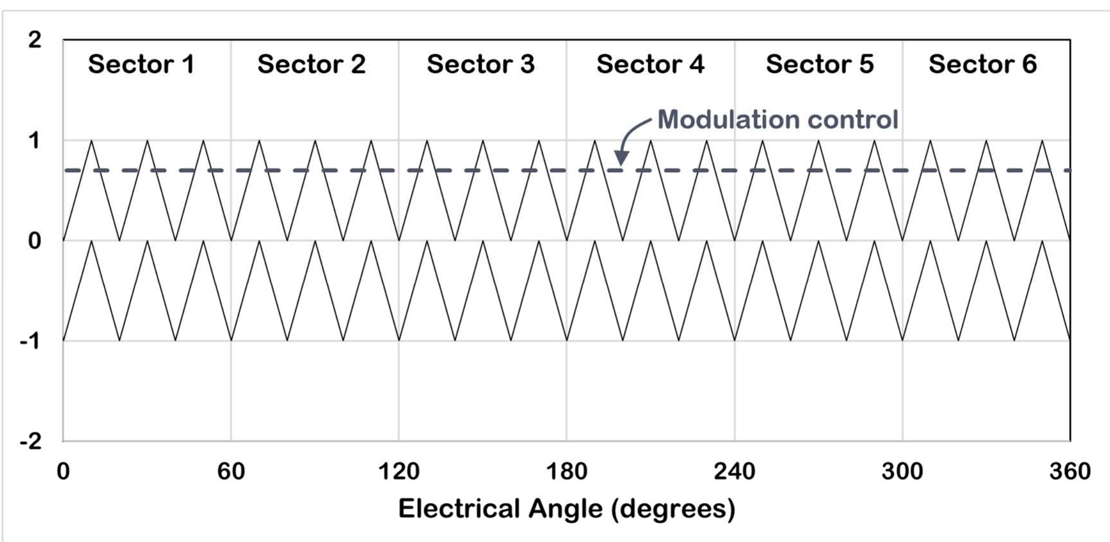

Fig. 3-6. Two carrier unipolar modulation control and carrier waveforms

The switching function is simply $\tau = M$, where again *M* is the ratio of the modulation control voltage to the peak of the corresponding carrier waveform. A small magnitude for modulation control results in narrow pulse widths. Enforcing a minimum pulse width, for example up to a few percent of the switching period, is a common best practice. This avoids back-to-back switching loss in the inverter

MOSFETs, which could otherwise cause inverter MOSFET failure, even though the power output is low. A common way to achieve this is by reducing the switching frequency from for example 20 kHz down to 4 kHz. This puts the switching frequency into the audible range, causing a humming sound. Pulse skipping is another approach, which results in a lower pitch growling sound.

A notable advantage of the two-carrier unipolar modulation method is a significant reduction in power loss in the inverter MOSFETs because of the reduced number of switching events. It is commonly used for BLDC motor control because it is the most efficient modulation method presented here both for the inverter and the motor.

3.4. Current and BEMF Sensing

Despite not fully utilizing the DC link voltage nor the motor's full torque capability, simple control combines with lower cost current sensing in applications requiring only speed control as opposed to precise speed and/or positioning control. Low cost and a long, maintenance-free service life explain the huge popularity of BLDC motors.

It is possible to implement trapezoidal control of a PMSM, and sinusoidal (field-oriented) control of a BLDC motor. However, a BLDC motor is optimized for trapezoidal control, and a PMSM is optimized for sinusoidal control.

As final note before moving on to field-oriented control of a PMSM, there are other possible modulation methods than the ones presented here. This is simply an introduction to the vast subject of pulse width modulation.

After reading this far, you may be relieved to know that Qorvo provides evaluation boards and pre-certified firmware that is compliant with UL / IEC60730 Class B safety standards. The intricate details of both trapezoidal and field-oriented control are already solved, which of course reduces design risk and time.

4. Field-Oriented Control of a PMSM

Field-oriented control (FOC), sinusoidal commutation, and sinusoidal control are all synonymous. FOC aligns stator fluxes to produce maximum torque per stator current, and it regulates the amplitude and fundamental frequency of sinusoidal phase currents. All three inverter legs have one switch position gated on at any given time (ignoring deadtime during switching), so the inverter and PMSM are fully utilized because each phase is always energized. DC link voltage is also fully utilized depending on the PWM method. The inverter is the same 2L-VSI as for BLDC motor drive, with each of the six switches allowing reverse current flow regardless of gate status.

4.1. Space Vector PWM in a Nutshell

The inverter is shown again in Fig. 4-1(a) with highlighted switch positions on and the others off, corresponding to one of eight allowed switch states. The NPN state is highlighted, where the N or P notation corresponds to the bottom or top switch gated on, respectively. Each switch state is easier to track with the use of a switch state map as shown in Fig. 4-1(b). This map is aligned with the magnetic axes of the PMSM, with axis designators corresponding to inverter legs in (a).

The map in Fig. 4-1(b) has six switch-state vectors, with each vector labelled with its corresponding switch state. Each of these vectors has a length of 2/3rds of the total DC link voltage, with the center of the state map representing the center point of the load, which is labelled '*s*' in the machine in Fig. 4-1(a). Consider the NPN state for example. With Q2 and Q6 on, phase *u* and *w* windings are parallel. By voltage division, the voltage across *u* and *w* windings is $\frac{1}{3} \cdot V_{bus}$, and the voltage across phase *v* winding is $\frac{2}{3} \cdot V_{bus}$, which is the length of the NPN state vector.

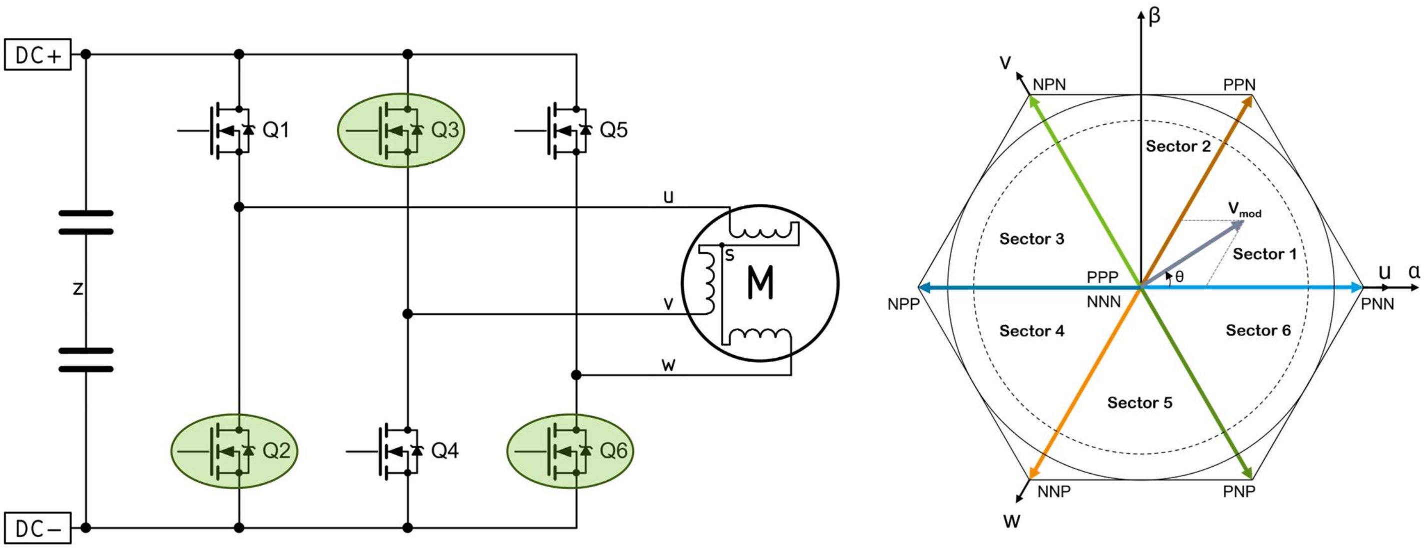

(a) (b)

Fig. 4-1. 2L-VSI (a) inverter highlighting NPN switch state, and (b) switch state map

The state vectors form the boundaries between six sectors, with each sector occupying a 60-degree wedge of the state map. With the DC link as the energy source, the inverter alternately applies line-to-line voltages to the PMSM. We note that flux is Volt-seconds, so the inverter creates rotating stator flux. There is a rotating modulation control vector, commonly called a reference vector, or reference voltage. Dashed lines show the projections of this vector onto the nearest state vectors. The PWM generator, gate drivers, and inverter approximate the modulation vector at the PMSM terminals by averaging time spent at nearby state vectors. For the modulation vector shown in Fig. 4-1, the nearest vectors are PNN, PPN, PPP, and NNN. These last two vectors are redundant zero vectors that short the motor terminals. The maximum modulation vector length without overmodulating is indicated by the circle inscribed in the hexagonal border of the state map. The radius of this circle is $\frac{2}{3} \cdot V_{bus} \cdot \cos(30\,°) = \frac{\sqrt{3}}{3} \cdot V_{bus} = 0.577 \cdot V_{bus}$. This is space vector PWM (SVM) “in a nutshell”. There are two common characteristics of SVM:

1. For a wye-connected load as in a PMSM, the load common point *must float* due to current interaction between phases. This is true for any modulation depth (modulation vector length). A floating load common point forces the sum of currents to be zero.
2. Full utilization of the DC link voltage is achieved by the variation in potential between the load common point and the DC link.

FOC is independent of PWM method. There are many types of SVM, all well documented, so they are not further reported here [3]. We note however, that sine-triangle PWM modulates each phase independently, so the load common point need not float. If accessible, it can connect to the center of a split DC link, which facilitates filtering electro-magnetic interference (EMI) at the expense of less utilization of the total DC link voltage. The dashed circle in Fig. 4-1(b) indicates the maximum modulation vector length (without overmodulation) of $\frac{1}{2} \cdot V_{bus}$ with sine-triangle PWM. SVM can apply 15% higher voltage to the machine terminals compared to sine-triangle PWM, allowing higher current and thus torque. Combine this with the fact that all three phases are always energized, as opposed to only two with trapezoidal control, and it becomes clear that a PMSM with FOC and SVM can deliver significantly more torque than a same-size BLDC machine with trapezoidal control. Torque ripple is also practically eliminated because there are no attempts to step change the current, and the average voltages applied to the PMSM are sinusoidal, closely matching the mostly sinusoidal BEMF.

4.2. Controller Functions Required for FOC

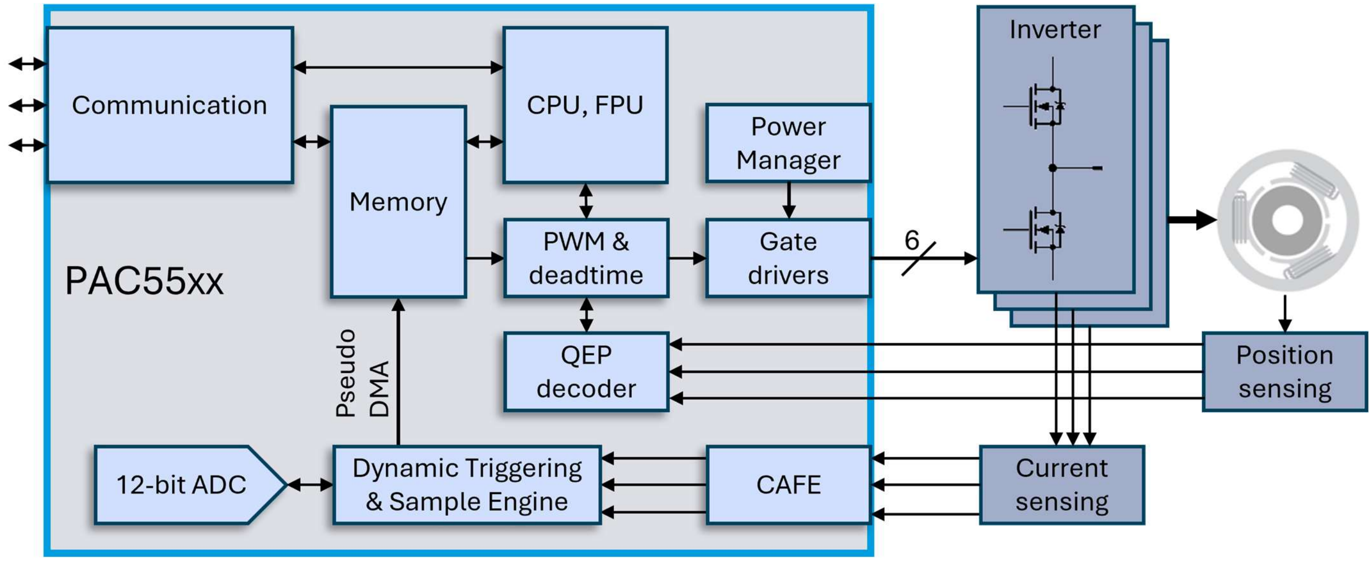

Fig. 4-2. PMSM drive block diagram showing Qorvo PAC MCD function blocks

Fig. 4-2 shows a PMSM drive block diagram including a Power Application Controller® that integrates all the above-mentioned functions plus more into a single integrated circuit. Current sensing is implemented with one to three current sense resistors in series with inverter phase legs and the DC- rail. Sensing all three phase currents allows checking whether their sum equals zero. If the sum is nonzero due to noise, it can be forced to zero by the MCU.

Inside the configurable analog front end (CAFE) are precision differential programmable gain amplifiers that condition the current sense signals, i.e., the voltage drop across the current sense resistors. Single-ended programmable gain amplifiers facilitate sensing DC link voltage, temperature, and other parameters. Overcurrent protection comparators with digital-to-analog converters provide both fast-acting and more filtered overcurrent protection. Simultaneous sample-and-hold, extremely fast analog-to-digital conversion, and hardware multiply & divide inside PAC55xx MCDs minimize delay-induced errors in FOC calculations. If position sensing is needed, such as in high-precision positioning, a QEP module decodes quadrature encoder signals. The PWM generator is the PWM & deadtime block. It includes safety logic from overcurrent comparators and other sources. The integrated power manager powers the internal high-side and low-side gate drivers and all internal circuitry.

4.3. Clarke Transformation

The Clarke transformation, also called alpha-beta transformation, results in a two-axis, stationary reference frame. This is possible because we force phase voltages and hence currents to balance, so they sum to zero and are 120° out of phase with each other.

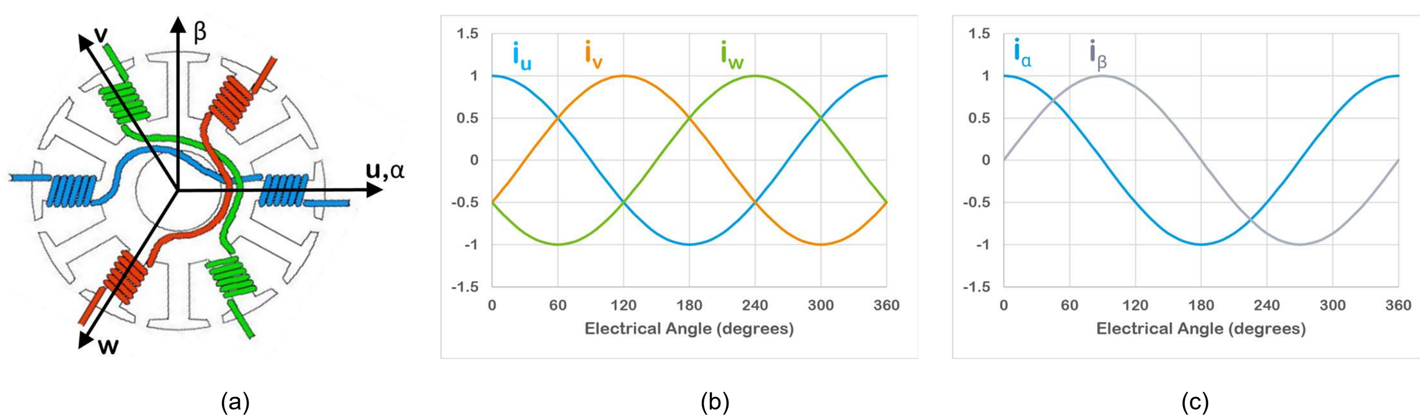

Fig. 4-3. (a) *uvw* and *αβ* axes on PM motor, (b) and phase *u*, *v*, and *w* current waveforms before and after (c) Clarke transformation

The equations of the vector magnitude invariant Clarke transformation are:

Forward: $\begin{bmatrix} f_\alpha \\ f_\beta \\ f_\gamma \end{bmatrix} = \frac{2}{3}\begin{bmatrix} 1 & -\frac{1}{2} & -\frac{1}{2} \\ 0 & \frac{\sqrt{3}}{2} & -\frac{\sqrt{3}}{2} \\ \frac{1}{2} & \frac{1}{2} & \frac{1}{2} \end{bmatrix}\begin{bmatrix} f_u \\ f_v \\ f_w \end{bmatrix}$ Inverse: $\begin{bmatrix} f_u \\ f_v \\ f_w \end{bmatrix} = \begin{bmatrix} 1 & 0 & 1 \\ -\frac{1}{2} & \frac{\sqrt{3}}{2} & 1 \\ -\frac{1}{2} & -\frac{\sqrt{3}}{2} & 1 \end{bmatrix}\begin{bmatrix} f_\alpha \\ f_\beta \\ f_\gamma \end{bmatrix}$

Here *f* is a general variable denoting current *i*, voltage *v*, flux linkage *λ*, or charge *q*. The magnitudes remain unchanged for input and output waveforms of this version of the Clarke transformation. Phase *u* and *α* are identical as shown in Fig. 4-3(b) and (c), and *α* and *β* are quadrature, meaning offset from each other by 90 degrees.

$f_\alpha = \frac{2}{3}f_u - \frac{1}{3}f_v - \frac{1}{3}v_w = \frac{3}{3}f_u - \frac{1}{3}f_u - \frac{1}{3}f_v - \frac{1}{3}f_w = f_u$ because quantities in a balanced three-phase system sum to zero. Finally, $f_\beta = \frac{f_v - f_w}{\sqrt{3}}$, and $f_\gamma = \frac{1}{2}(f_u + f_v + f_w) = 0$. We therefore ignore the *γ* axis, so the result is effectively a 3-to-2 axes transformation.

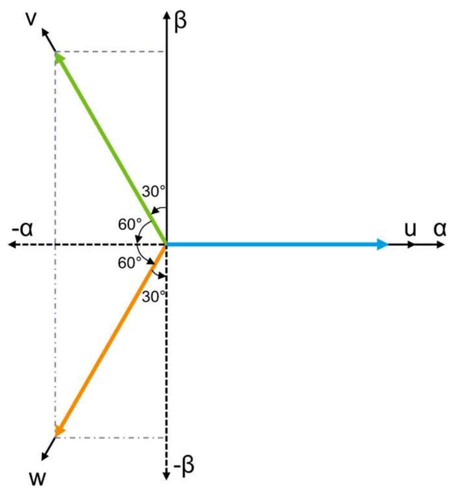

Fig. 4-4. *uvw* projections onto *αβ* axes on the $f_u + f_v + f_w = 0$ plane

The *αβ* axes lie on a plane defined by $f_u + f_v + f_w = 0$, but the *uvw* axes are not on this plane, as evident by the nonzero bottom row of the Clarke transformation. The projections of *uvw* axes onto the *αβ* plane are depicted as vectors in Fig. 4-4.

Suppose the *uvw* vectors are currents. Summing them we have $i_\alpha = i_u - i_v\cos(60°) - i_w\cos(60°) = i_u - \frac{1}{2}i_v - \frac{1}{2}i_w$, which matches the top row of the forward Clarke matrix. Vector projections onto the *β* axis are: $i_\beta = i_u \cdot 0 + i_v\sin(60°) - i_w\sin(60°) = i_u \cdot 0 + \frac{\sqrt{3}}{2}i_v - \frac{\sqrt{3}}{2}i_w$, which matches the second row of the Clarke matrix. $i_\gamma = \frac{1}{2}i_u + \frac{1}{2}i_v + \frac{1}{2}i_w = 0$ because of balanced 3-phase operation as already mentioned. Why is there a $\frac{2}{3}$ factor in the Clarke transformation? This is because the *uvw* axes are not on the *αβ* plane, and the $\frac{2}{3}$ factor keeps the magnitude of the waveform peaks (vectors along the axes) equal before and after the transformation, as seen in Fig. 4-3(b) and (c).

There is an alternate form of the Clarke transformation called power invariant, which is identical to the vector magnitude invariant form except for a $\sqrt{\frac{2}{3}}$ factor instead of $\frac{2}{3}$ and each element of the third row (*γ* coefficients) is $\frac{1}{\sqrt{2}}$ instead of $\frac{1}{2}$. In either case, the third row is usually omitted because values on the *γ* axis sum to zero.

A final observation is that the magnetic field corresponding to a phase current is in the same direction as the current. This is more easily visualized by imagining the right-hand rule applied to Fig. 4-3(a) (and that the stator windings are wound the corresponding way). For example, imagine wrapping the fingers of your right hand around the phase *u* winding so that your fingers point in the direction of current flow in the winding. Your right thumb then points in the direction of both current flowing in phase *u* and the resulting magnetic field. This insight becomes important as we consider the Park transformation.

4.4. Park Transformation

The Park transformation, also called *dq* transformation, results in a two-axis rotating reference frame. The same simplification from balanced 3-phase operation applies here, so we ignore the 0 axis. It is always zero because there is no common-mode current or direct current in the motor windings.

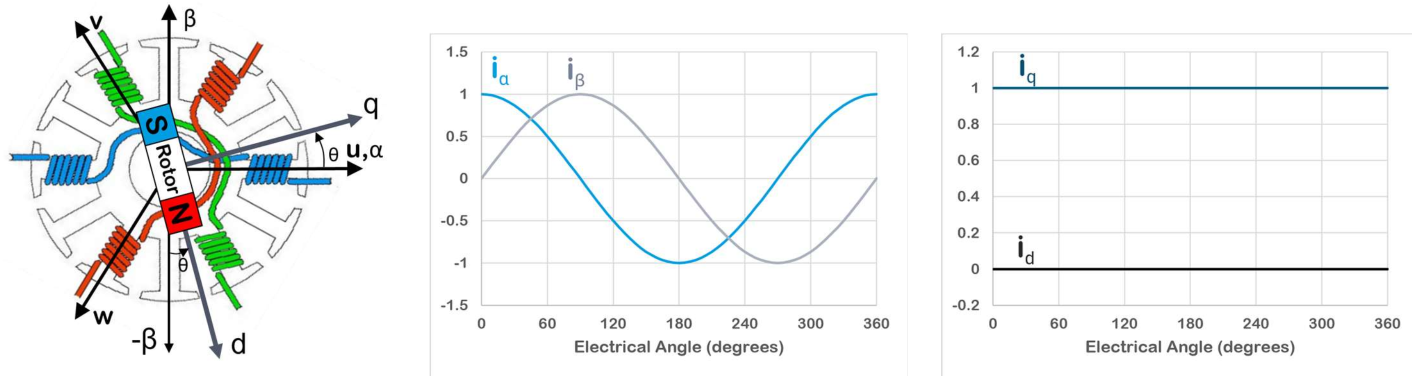

(a) (b) (c)

Fig. 4-5. (a) *αβ* and *dq* axes on PMSM, (b) *α* and *β* current waveforms before and after (c) Park transformation

There are (unfortunately) different definitions of the *dq* axes with respect to the *αβ* axes. Here we use the convention that the *q* axis aligns with the projection of the *u* axis (same direction as the *α* axis) onto the *dq* plane when the electrical rotation angle *θ* is zero [4]. The *d* axis is 90° clockwise from the *q* axis. (It is sometimes drawn 90° counterclockwise from the *q* axis, or with the *d* and *α* axes aligned, which is unconventional.) The *dq* plane is coplanar with the *αβ* plane because both the *γ* axis and *0* axis values sum to zero. With this convention, sequence *d-q-0* forms a right-hand set. Imagine pointing the fingers of your right hand in the direction of the *d* axis, then curling your fingers toward the *q* axis. Your thumb then points in the direction of the *0* axis, which is perpendicular to the *dq* plane. Now we imagine rotating the *dq* axes along the *0* axis. With the *dq* axes and electrical angular velocities equal, the rotating *dq* axes form a synchronous reference frame.

With the *d* axis aligned with the rotor flux as indicated in Fig. 4-5(a), regulating all stator current to be along the *q* axis and zero along the *d* axis delivers maximum torque per stator current in a synchronous machine because the stator flux (aligned with the *q* axis) is at a right angle to the rotor flux. The resulting torque is counterclockwise. Regulating current along the *-q* axis causes maximum clockwise torque per stator current.

The Park transformation is a rotated Clarke transformation:

Forward: $\begin{bmatrix} f_q \\ f_d \\ f_0 \end{bmatrix} = \begin{bmatrix} \cos(\theta) & \sin(\theta) & 0 \\ \sin(\theta) & -\cos(\theta) & 0 \\ 0 & 0 & 1 \end{bmatrix} \cdot \begin{bmatrix} f_\alpha \\ f_\beta \\ f_\gamma \end{bmatrix}$ Inverse: $\begin{bmatrix} f_\alpha \\ f_\beta \end{bmatrix} = \begin{bmatrix} \cos(\theta) & \sin(\theta) \\ \sin(\theta) & -\cos(\theta) \end{bmatrix} \begin{bmatrix} f_q \\ f_d \end{bmatrix}$, ignoring *γ* and *0* axes.

The Park transformation is a 3-to-3 axis transformation but usually reduced to 2-by-2 because we ignore the *γ* and *0* axes as already mentioned. The trigonometric relationships are easier to visualize in Fig. 4-6.

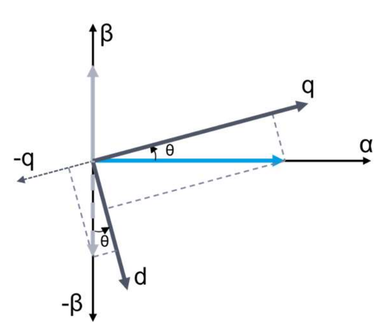

Fig. 4-6. *αβ* axes and rotating *dq* axes on the *dq* plane

The Park transformation includes sine and cosine functions that require the electrical angle (rotor flux angle). This allows alignment of the *d* axis with the rotor flux, as indicated by the magnet in Fig. 4-5(a). Torque is proportional to current along the *q* axis, and *d* axis current is set to zero for maximum torque per motor current. Control variables are steady (not periodic functions) as seen in Fig. 4-5(c). They are also inherently stable and so are easy to process with proportional-integral (PI) controllers.

4.5. FOC Calculations

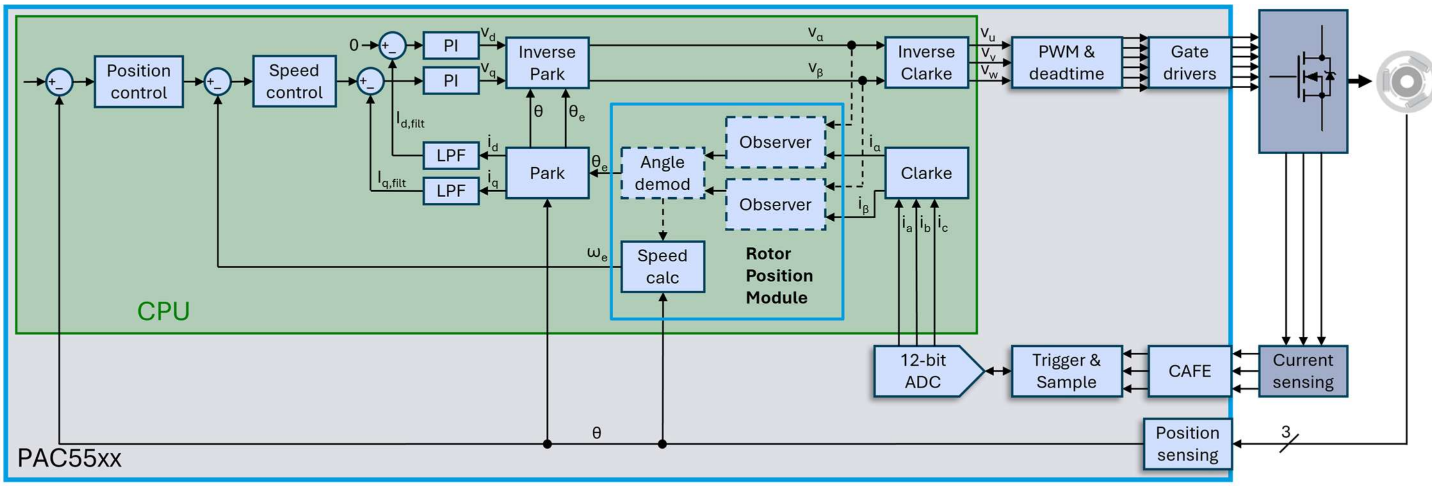

Fig. 4-7. FOC calculations highlighted by the green rectangle inside an integrated MCD

Field-oriented control (FOC) always requires feedback of at least two phase currents. Often all three are sampled to mitigate noise by checking whether their sum equals zero. If it is nonzero, it is due to noise and/or current measurement errors. Most Qorvo MCDs can simultaneously sample all three phase currents, and then each sample is digitized in as little as 400 ns. The synchronized current measurements go through the Clarke transformation, resulting in alpha-beta currents. The rotor position module uses these along with feedforward signals v_α and v_β to calculate rotor flux angle and angular velocity. Rotor position library functions available from Qorvo handle both position feedback and sensorless control. Various methods can be used to estimate rotor position θ and speed ω. Shown Fig. 4-7 are two observers and an angle demodulator. Motor parameters, namely stator winding resistance and inductance, are required. Knowing the rotor flux angle, the Park transformation yields i_d and i_q in the synchronous reference frame. These become v_d and v_q after filtering and PI controllers. An inverse Park transformation yields v_α and v_β, which after an inverse Clarke transformation become 3-phase reference voltages needed by the PWM generator. All these computations execute extremely fast in the PAC55xx with its 150 MHz Arm Cortex CPU with single cycle multiply & divide and floating point unit.

4.6. Autotuning

The rotor position module outlined in Fig. 4-7 is also known as an estimator. The required parameters are usually available in the PMSM datasheet. If they are unavailable or incorrect for any reason, Qorvo firmware functions can determine the parameters, allowing optimal control. PI controllers also require tuning. Again, this is accomplished by Qorvo firmware functions.

Fig. 4-8 and Fig. 4-9 show control parameters and phase current of a PMSM with a sudden torque change. In each figure, channel 1 (yellow) = output from speed PI controller, channel 2 (blue) = estimated speed, channel 3 (purple) = output from i_q PI controller, channel 4 (green) = phase current. In Fig. 4-8, the proportional and integral gains are too low in the i_d and i_q PI controllers. Response is slow, and parameters are “hunting”, not settling to steady-state values.

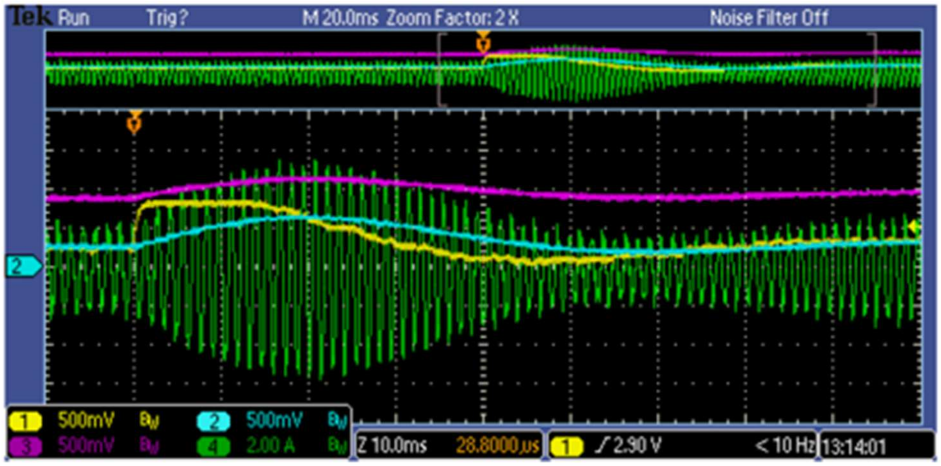

Fig. 4-8.PMSM response to sudden torque change with PI controllers out of tune

To remedy the poor response, autotuning functions adjusted the PI controller gains. The result is shown in Fig. 4-9. Response to the torque step change is rapid, and parameters quickly settle to steady-state values.

Fig. 4-9. PMSM response to sudden torque change after autotuning PI controllers

5. Summary

A PM motor drive system has four building blocks: power source, highly integrated motor controller & driver, inverter, and PM motor.

The ubiquitous 2L-VSI was introduced to drive both brushless DC and permanent magnet synchronous machines. Motor construction is similar, but there are notable differences. A BLDC motor has a somewhat trapezoidal shaped BEMF, whereas the PMSM BEMF is sinusoidal. These match with the intended control method. Trapezoidal BLDC control was presented along with three PWM methods. Unipolar with two carriers is the most efficient and popular modulation method presented here both for the inverter and the motor.

A BLDC motor drive is low cost because of fewer current sensors, if any. It is also simpler to control. Its main drawback is torque ripple, making it suited for speed control applications such as many power tools, pumps, fans, etc. PMSM with FOC has no torque ripple, higher torque capability, and full utilization of DC link voltage. PMSM with FOC is good at everything, including precise speed and position control. Sensorless control is an option for both.

Understanding Clarke and Park transformations is necessary to clarify how FOC works. FOC calculations were outlined, and autotuning simplifies drive development.

References

[1] D. Graham Holmes, Thomas A. Lipo; “Modulation of Three-Phase Voltage Source Inverters,” in *Pulse Width Modulation for Power Converters, Principles and Practice*,Piscataway, NJ, USA: IEEE Press / Wiley InterScience, 2003, ch. 5, sec. 5.6, pp. 251-253.

[2] D. Graham Holmes, Thomas A. Lipo; “Zero Space Vector Placement Modulation Strategies,” in *Pulse Width Modulation for Power Converters, Principles and Practice*,Piscataway, NJ, USA: IEEE Press / Wiley InterScience, 2003, ch. 6, sec. 6.7, pp. 302-310.

Revision History

Revision	Author	Date	Description
A	Jonathan Dodge, P.E.	9 Feb. 2026	Initial draft

Contact Information

For the latest specifications, additional product information, worldwide sales and distribution locations:

Web: www.qorvo.com

Tel: +1 844-890-8163

Email: customer.support@qorvo.com

Important Notices